https://doi.org/10.5194/egusphere-2025-2536
Preprint. Discussion started: 23 June 2025

Assessing the efficacy of river-based ocean alkalinity enhancement for carbon sequestration under high emission pathways

Xiao-Yuan Zhu[1], Shasha Li[1], Wei-Lei Wang[1*]

[1] State Key Laboratory of Marine Environmental Science & College of Ocean and Earth Sciences, Xiamen University, Xiamen 361102, China

Correspondence to: Wei-Lei Wang (weilei.wang@xmu.edu.cn)

Abstract. Among various proposed geoengineering methods, ocean alkalinity enhancement (OAE) stands out as a unique solution. By mimicking natural weathering processes, OAE can simultaneously enhance oceanic carbon uptake and mitigate ocean acidification. However, the full efficacy and potential side effects of OAE remain to be fully understood. To evaluate the efficacy of OAE through natural pathways via rivers, we applied a 5-fold alkalinity flux increase (OWE5) at the mouths of global rivers from 2020 to 2100 in a fully coupled Earth System Model under a high-emission scenario (SSP585). In additional sensitivity tests, the flux was increased to 7.5- (OWE75), 10-fold (OWE10), or restored to the control level (OWE0) in 2050. Compared to the control run, global mean surface pH increased by 0.02, 0.03, 0.04, and 0.006; the oceanic inventory of dissolved inorganic carbon (DIC) increased by 5.39, 7.41, 9.50, and 2.06 Pmol; and atmospheric CO_2 concentration decreased by 29, 40, 51, and 11 ppmv under OWE5, OWE75, OWE10, and OWE0, respectively, by the end of the century. The most significant responses to OAE were observed in coastal regions, as well as in the Indian and North Atlantic Oceans. Our simulations demonstrate that OAE via rivers is an effective and practical method, however, even a tenfold increase in alkalinity flux is insufficient to reverse the trends of ocean acidification or rising atmospheric CO_2 levels under a high-emission scenario. This underscores the urgent need for complementary technological innovations and aggressive emission reduction strategies to curb CO_2 emissions.

Short Summary. Ocean Alkalinity Enhancement (OAE), a geoengineering method that mimics the natural weathering mechanism, is the only Carbon Dioxide Removal methods that can simultaneously absorb CO_2 and alleviate ocean acidification. In this study, we evaluated the effectiveness of riverine OAE under high emission scenario in a fully coupled Earth System Model. The simulations show the riverine OAE effectively boosts ocean carbon uptake and partially combats ocean acidification, but continuous OAE is necessary to achieve the desired outcomes.

1 Introduction

Since the Industrial Revolution, rising atmospheric carbon dioxide (CO_2) levels have driven dramatic climate change—one of the greatest challenges we are facing today. Global average sea surface temperature has already increased by 1.1 °C relative to the 1850–1900 baseline (IPCC, 2023) and continues to rise, approaching the Paris Agreement's target of limiting warming to

https://doi.org/10.5194/egusphere-2025-2536
Preprint. Discussion started: 23 June 2025

below 1.5 °C by the end of this century (UNFCCC, 2015). Excessive warming has triggered increasingly frequent and intense extreme events, such as marine heatwaves, polar ice melt, and sea level rise, posing severe risks to both human societies and marine ecosystems. As a major carbon sink, the ocean has absorbed approximately one-third of anthropogenic CO_2 emissions since the Industrial Revolution (Friedlingstein et al., 2023). However, this uptake has led to ocean acidification, which lowers the saturation state of calcium carbonate and threatens calcifying organisms such as corals, foraminifera, and other marine species (Beaufort et al., 2011; Kleypas et al., 1999; Riebesell et al., 2000; Zeebe et al., 2008). Whether through global warming or ocean acidification, the impacts of CO_2 emissions on the climate system are becoming increasingly severe, underscoring the urgent need to reduce atmospheric CO_2 concentrations.

Emission reduction and carbon sequestration are two complementary strategies for lowering atmospheric CO_2 concentrations and should be pursued in tandem to effectively mitigate climate change and minimize socioeconomic impacts. For emission reduction, technological innovation is needed to transition away from high-emission energy sources. However, even under the RCP2.6 scenario—which includes aggressive mitigation and negative emissions of 0.5–3 Gt C yr^{-1}—an estimated 50–250 Gt C of carbon storage capacity will still be required by the end of this century (Gasser et al., 2015). This underscores that deep emission cuts alone will not suffice to achieve carbon neutrality. Therefore, additional technologies must be developed to actively remove CO_2 from the atmosphere—a set of approaches collectively known as Carbon Dioxide Removal (CDR).

To date, several CDR methods have been proposed and evaluated, both theoretically and at small experimental scales, for their effectiveness in removing atmospheric CO_2 (Keller et al., 2014). As the largest carbon reservoir on Earth, the ocean holds significant potential for enhanced CO_2 uptake. This has led to increasing interest in marine-based CDR (mCDR) approaches. Proposed mCDR strategies include large-scale afforestation of coastal and marine ecosystems (Duarte et al., 2022; Wang et al., 2023), artificial ocean upwelling (Jürchott et al., 2023), ocean alkalinity enhancement (OAE; Eisaman et al., 2023; Oschlies et al., 2023; Renforth & Henderson, 2017), and micronutrient fertilization (Bach et al., 2023; Lampitt et al., 2008). Among these, OAE is particularly promising because it offers the dual benefit of reducing atmospheric CO_2 and alleviating ocean acidification, making it an ideal candidate for mitigating CO_2-driven climate impacts through mCDR.

Alkalinity is defined as the sum of the net concentrations of hydrogen ion (H^+) acceptors in seawater. Approximately 95% of seawater alkalinity is contributed by the carbonate system, primarily in the form of carbonate and bicarbonate ions. A decline in surface alkalinity, driven by enhanced upper-ocean stratification, has been shown to reduce oceanic carbon uptake (Chikamoto et al., 2023). OAE works by introducing carbonate, bicarbonate, or other H^+ acceptors into surface waters, thereby increasing carbonate ion concentrations, removing excess H^+, raising pH, and reducing the partial pressure of CO_2 (pCO_2) in seawater. This strengthens the

https://doi.org/10.5194/egusphere-2025-2536
Preprint. Discussion started: 23 June 2025

air–sea CO_2 disequilibrium, leading to greater oceanic CO_2 uptake and, ultimately, a decrease in atmospheric CO_2 concentrations.

Many laboratory and field experiments have assessed the carbon capture potential of OAE, and the biological feedback associated with it (González-Santana et al., 2023; Guo et al., 2023; Montserrat et al., 2017). A wide range of materials has been tested as alkalinity sources, including sodium carbonate, powdered lime, olivine sand, and steel slag. For instance, a mesocosm experiment using sodium carbonate/bicarbonate salts was conducted in coastal waters to investigate potential effects on trace metal cycling and phytoplankton physiology (González-Santana et al., 2023). The results indicated that sodium salt addition did not alter iron dynamics. Another study applying olivine and steel slag to coastal waters found that these materials increased alkalinity by 29 and 361 µmol kg^{-1}, respectively, which enhanced CO_2 storage capacity in seawater by 0.9% and 14.8% (Guo et al., 2023). Regarding alkalinity stability, experiments have shown that CO_2-equilibrated alkaline solutions pose the lowest risk of alkalinity loss to the deep ocean (Hartmann et al., 2023). However, such studies primarily demonstrate local and theoretical outcomes. Comprehensive understanding of the global ocean's response to OAE remains limited.

To address this, recent studies have employed Earth System Models (ESMs) to explore OAE responses at a global scale. For example, a global-scale ocean circulation model coupled with a biogeochemical module simulating olivine dissolution suggested that OAE helps oceanic carbon sequestration, with a particle size of ~1 µm required for full dissolution before sinking to the deep ocean (Köhler et al., 2013). Another centennial-scale simulation tested a fixed 2:1 ratio of alkalinity addition to CO_2 emissions, demonstrating that such alkalinization could maintain surface ocean pH and carbonate chemistry near present-day values (Ilyina et al., 2013). A study using a fully coupled ESM found that applying 0.25 Pmol Alk yr^{-1} from 2020 to 2100 could reverse ocean acidification and offset atmospheric CO_2 increases under low-emission (RCP2.6) scenarios, though significantly more alkalinity would be needed under high-emission (RCP8.5) scenarios (Lenton et al., 2018). However, most model-based studies assume a uniformly distributed and constant-rate alkalinity addition across the global ocean—an assumption that is unlikely to be achievable in practice.

On geological timescales, alkalinity is naturally added to the ocean via chemical weathering of rocks on land, with river systems acting as the primary delivery pathway (Fig. 1). Though slow, this natural process plays a crucial role in regulating Earth's long-term climate. To mimic this mechanism, we use a state-of-the-art, fully coupled Earth System Model to evaluate a riverine-based, global-scale OAE scenario under a high-emission pathway (Shared Socioeconomic Pathway 5-8.5, SSP585). Specifically, we simulate enhanced natural weathering by increasing riverine alkalinity fluxes by factors of 5, 7.5, and 10. To investigate the potential for climate rebound and the persistence of CO_2 uptake following the cessation of OAE, we halt alkalinity addition in 2050 and extend the simulation through 2100. Finally, we assess how this natural

https://doi.org/10.5194/egusphere-2025-2536
Preprint. Discussion started: 23 June 2025

weathering-based OAE strategy affects oceanic CO_2 uptake, surface carbonate chemistry, and the spatial redistribution of alkalinity and dissolved inorganic carbon (DIC).

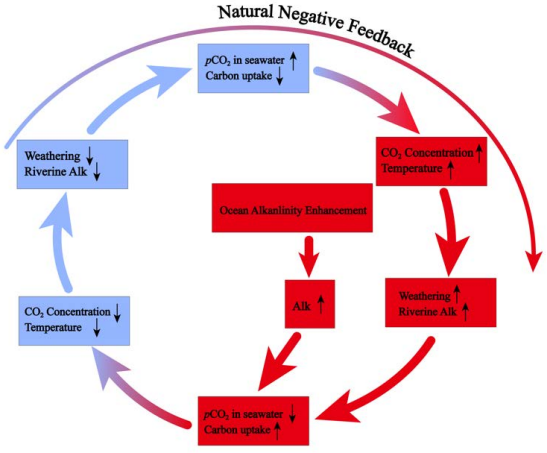

Figure1: Schematic diagram of natural negative feedback and OAE mechanism.

2 Methods

2.1 Model description

This investigation uses Community Earth System Model 2 (CESM2, https://www.cesm.ucar.edu/models/cesm2), a state-of-the-art, community-developed, fully-coupled earth system model consisting of ocean, atmosphere, land, sea-ice, river, and wave models through a coupler to exchange states and fluxes (Danabasoglu et al., 2020). The atmospheric component in this study is the Community Atmosphere Model Version 6 (CAM6) with a general resolution of $0.9° \times 1.25°$. The ocean component uses the Parallel Ocean Program Version 2 (POP2; Smith et al., 2010) with a horizontal resolution of nominal 1° (gx1v7) and 60 vertical levels. The biogeochemical component is MARBL, a prognostic ocean biogeochemistry model with a coupled cycle of carbon, macronutrients (nitrogen, phosphorus, silicate), iron, and oxygen (Long et al., 2021).

In CESM, all tracers in ocean follow the prognostic governing equation:

$$\frac{\partial \chi}{\partial t} + \nabla \cdot (u \cdot \chi) - \nabla \cdot (K \nabla \chi) = J_\chi(X),$$

where the term on the left calculates the time-tendency, advection and diffusion, and the term on the right calculate the sum of the sources and sinks.

https://doi.org/10.5194/egusphere-2025-2536
Preprint. Discussion started: 23 June 2025

The river input of alkalinity is set as an external forcing on the estuary grids. The intensity of fluxes is based on the GlobalNEWS (Mayorga et al., 2010) and IMAGE-GNM (Beusen et al., 2015) datasets. There are two forms of inorganic carbon input into ocean module, DIC and alkalinity. Riverine DIC inputs are assumed in the form of bicarbonate (HCO_3^-), alkalinity flux is therefore equal to DIC influx. Readers are referred to Long et al. (2021) for more details.

The source and sink term of alkalinity in CESM include the utilization of nitrate and ammonia, the formation and dissolution of $CaCO_3$, and release by zooplankton grazing, as shown in the following equation:

$$\mathrm{ALK}_{\mathrm{tendency}} = -\mathrm{I}_{\mathrm{NO}_3} + \mathrm{I}_{\mathrm{NH}_4} + 2 * \mathrm{CaCO}_{3_{\mathrm{remi}}} + 2 * (\mathrm{G} - \mathrm{F}) ,$$

where the term I_{NO3} and I_{NH4} indicate the interior tendency of nitrate and ammonia, $\mathrm{CaCO}_{3_{\mathrm{remi}}}$ means the dissolution of calcium carbonate, G means grazing-released alkalinity, and F means the formation of $CaCO_3$ by small phytoplankton.

2.2 Experiment design

We use prognostic CO_2 settings to explore the responses of climate to OAE. In such a setting, transient rather than prescribed CO_2 is used for the computations of both biogeochemistry modules and the atmospheric radiation to avoid the uncertainty that stems from the difference between responsive and prescribed atmospheric CO_2 forcing in ocean (Tyka, 2025). The model is spun up under the pre-industrial condition (esm-piControl), which is representative of the period before the onset of large-scale industrialization with the year of 1850 as the reference year. When the climate is balanced with forcing, the historical simulation is performed as an emission-driven simulation using the historical atmospheric CO_2 concentrations (esm-hist) prescribed by CMIP6 protocol till the year of 2014. After that, the system is forced by an emission-driven future scenario (SSP-based RCP ssp-585, esm-ssp585(Jones et al., 2016)) till 2100. Restart files in 2020 provided by the data manager of NCAR in the official CESM forum are used (https://bb.cgd.ucar.edu/cesm/). We first run a default simulation under esm-ssp585 from 2020 to 2100 as our control simulation (CTL hereafter). Then, we restart our simulation from 2020 to apply three OAE simulations and a termination of OAE in 2050. The detailed simulations are as follows:

Exp1: 5-fold fluxes enhancement of alkalinity till 2100 (OWE5).

Exp2: 7.5-fold fluxes enhancement of alkalinity based on OWE5 (OWE75) from 2050.

Exp3: 10-fold fluxes enhancement of alkalinity based on OWE5 (OWE10) from 2050.

Exp4: Termination of alkalinity enhancement (OWE0) based on OWE5 from 2050.

https://doi.org/10.5194/egusphere-2025-2536
Preprint. Discussion started: 23 June 2025

All alkalinity is added from rivers as a forcing in the model. To simplify the process, we do not change the parameters in the model but directly changed the fluxes from riverine sources. The globally integrated alkalinity fluxes are 0.11 Pmol/yr, 0.16 Pmol/yr and 0.22 Pmol/yr for OWE5, OWE75, and OWE10, which is respectively 0.088 Pmol, 0.14 Pmol, and 0.20 Pmol per year higher than the control run. Location of river mouths are shown in Fig. 2.

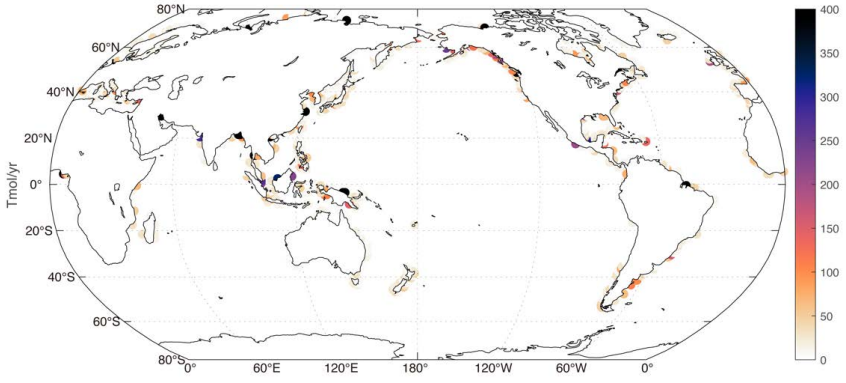

Figure 2: Location and fluxes of enhanced alkalinity input.

3 Results

3.1 Responses of upper 100 m mean alkalinity to alkalinity enhancement

Compared to the control run, mean alkalinity in the upper 100 m increases throughout the simulation phase under the OWE5 treatment (Fig. 3a). By the end of 2100, it has risen by 53 meq/m³ relative to the control, demonstrating the effectiveness of alkalinity enhancement. The OWE75 and OWE10 treatments show even larger increases—77 and 102 meq/m³, respectively (Fig. 3a). Although alkalinity begins to decline after the termination of addition in 2050, the OWE0 scenario still maintains elevated alkalinity levels compared to the control run through 2100.

Globally, OAE treatments result in increased alkalinity with notable spatial variability. The largest increases occur in coastal regions and the Arctic Ocean under the OWE5 treatment, reflecting the strong influence of riverine alkalinity inputs (Fig. 4b). Beyond these areas, significant increases are observed in the Atlantic and Indian Oceans, with the Subpolar North Atlantic (SPNA) showing the highest open-ocean response. In contrast, increases in the Pacific and Southern Oceans are comparatively smaller. The spatial patterns in OWE75 are generally like those of OWE5 (Fig. 4b, c). Under OWE10, however, alkalinity spreads further into subtropical regions (Fig. 4d), with particularly strong increases in the Indian Ocean and the

https://doi.org/10.5194/egusphere-2025-2536
Preprint. Discussion started: 23 June 2025

tropical and subtropical Atlantic compared to OWE5 and OWE75. Although more modest, even the subpolar Pacific begins to show a noticeable increase under OWE10. Overall, OWE10 exhibits the strongest alkalinity enhancement of all the treatments. While OWE0 results in a smaller alkalinity increase in the SPNA compared to other scenarios, this region still exhibits the most pronounced enhancement relative to the control run (Fig. 4e).

Vertically, alkalinity penetrates deeper in the Northern Hemisphere than in the Southern Hemisphere, likely due to two factors: (1) greater riverine alkalinity input in the north, and (2) subduction of alkalinity along with deep water formation in the high-latitude North Atlantic (Fig. 5). In all OAE treatments, the positive alkalinity anomaly rarely extends below 500 m in the Southern Hemisphere but can reach depths exceeding 1500 m around 50°–60°N (Fig. 5a–c). The polar and subpolar North Atlantic also show the sharpest vertical gradients, with alkalinity varying by more than 100 meq/m³ from the surface to 200 m in all three OAE scenarios.

Although alkalinity addition ceases after 2050 in the OWE0 simulation, a positive alkalinity anomaly persists through 2100, reaching depths of 1500 m near 50°–60°N. However, the magnitude of this increase is much smaller compared to the continuous addition scenarios (Fig. 5d), due to the cessation of external alkalinity supply. This difference is especially noticeable in regions with strong anomalies under OWE5, such as the subpolar North Atlantic (Fig. 5e).

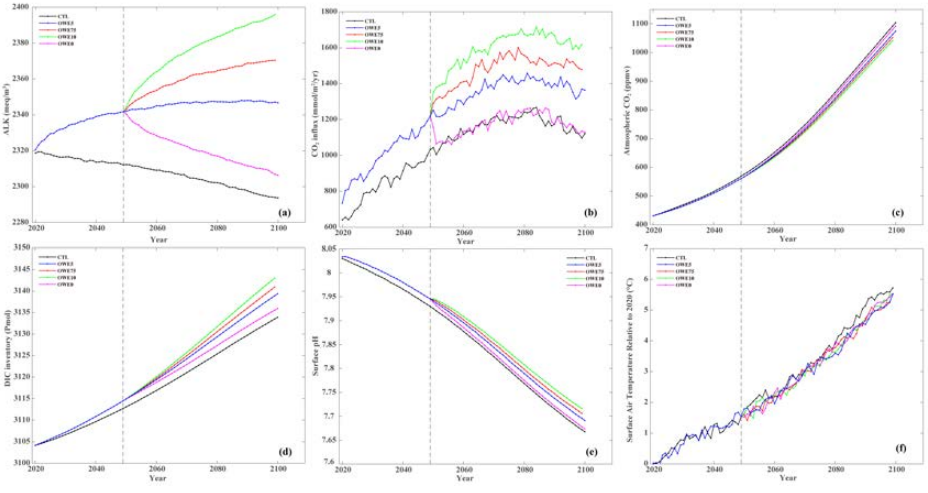

Figure 3: Global changes of (a) upper 100 m mean alkalinity (unit: meq/m^3), (b) CO_2 influx (unit: mmol/m^2/yr), (c) atmospheric CO_2 (unit: ppmv), (d) integrated DIC inventory (unit: Pmol), (e) surface pH, (f) surface air temperature (unit: ºC). Dash lines starting from in the year 2050 denote the onset of the 7.5×, 10× alkalinity enhancement scenarios, as well as the termination of alkalinity addition via rivers.

https://doi.org/10.5194/egusphere-2025-2536
Preprint. Discussion started: 23 June 2025

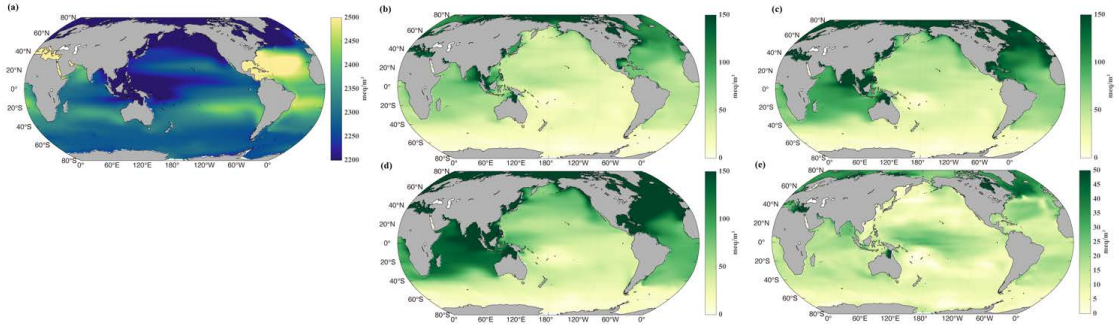

Figure 4: Distribution of alkalinity (unit: meq/m^3) in upper 100 m. (a) upper 100 m mean alkalinity in control simulation at the end of this century, (b) differences between OWE5 and CTL, (c) differences between OWE75 and CTL, (d) differences between OWE10 and CTL, (e) differences between OWE0 and CTL. Note the different colour scale of (e).

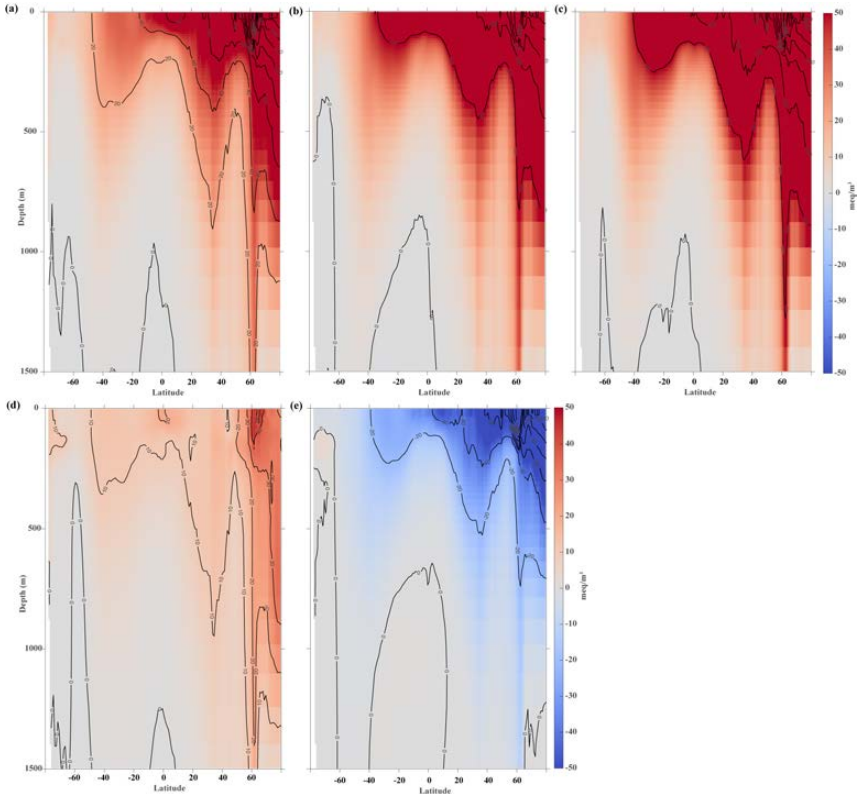

Figure 5: Vertical distribution of alkalinity anomaly (upper 1500 m). (a) differences between OWE5 and CTL, (b) differences between OWE75 and CTL, c) differences between OWE10 and CTL, (d) differences between OWE0 and CTL, (e) differences between OWE0 and OWE5.

https://doi.org/10.5194/egusphere-2025-2536
Preprint. Discussion started: 23 June 2025

3.2 CO_2 absorption after alkalinity enhancement

The OAE treatments result in a reduction of surface seawater pCO_2, indicating an increased disequilibrium between atmospheric and oceanic pCO_2 compared to the control run (Fig. 6). This enhanced disequilibrium facilitates greater oceanic CO_2 uptake. In all OAE scenarios, surface pCO_2 decreases significantly in coastal regions, where alkalinity is most strongly enhanced. The pCO_2 reduction also spreads into the open ocean and even reaches the Southern Ocean, despite its distance from riverine inputs (Fig. 6b–d). The magnitude of pCO_2 reduction is greater in simulations with higher alkalinity additions, demonstrating a strong positive relationship between alkalinity enhancement and oceanic CO_2 uptake. In the OWE0 simulation, where alkalinity addition is halted in 2050, surface pCO_2 remains slightly lower than in the control run even 50 years later (Fig. 6e). In OWE5, OWE75, and OWE10, surface pCO_2 decreases by more than 20 ppmv compared to the control, with OWE10 showing the greatest reduction. In contrast, OWE0 achieves only a ~10 ppmv decrease by 2100. These results highlight the importance of continuous alkalinity addition to sustain enhanced CO_2 uptake by the ocean.

The reduction in surface pCO_2 drives an increase in oceanic CO_2 influx (Fig. 3b). Under the SSP585 scenario, the CTL exhibits a steady increase in CO_2 uptake until around 2080, followed by a gradual decline. In contrast, all OAE treatments show accelerated CO_2 influx from the start of alkalinity addition through the end of the simulation (Fig. 3b). In OWE75 and OWE10, where alkalinity is increased further in 2050, the rate of CO_2 uptake accelerates even more compared to OWE5. However, a decline in CO_2 influx after 2080 is still observed across all OAE scenarios, although it is less pronounced than in the control run. When alkalinity addition ceases in 2050 (OWE0), the CO_2 influx eventually returns to the same rate as in the control simulation (Fig. 3b).

This enhanced oceanic CO_2 uptake leads to a reduction in atmospheric CO_2 concentrations (Fig. 3c). By 2100, the control simulation projects atmospheric CO_2 levels to reach 1104 ppmv. In comparison, OAE treatments lower atmospheric CO_2 by 29 ppmv (OWE5), 40 ppmv (OWE75), and 51 ppmv (OWE10), corresponding to reductions of approximately 2.7%, 3.6%, and 4.6%, respectively. Even the OWE0 scenario results in an 11 ppmv decrease relative to the control by the end of the century.

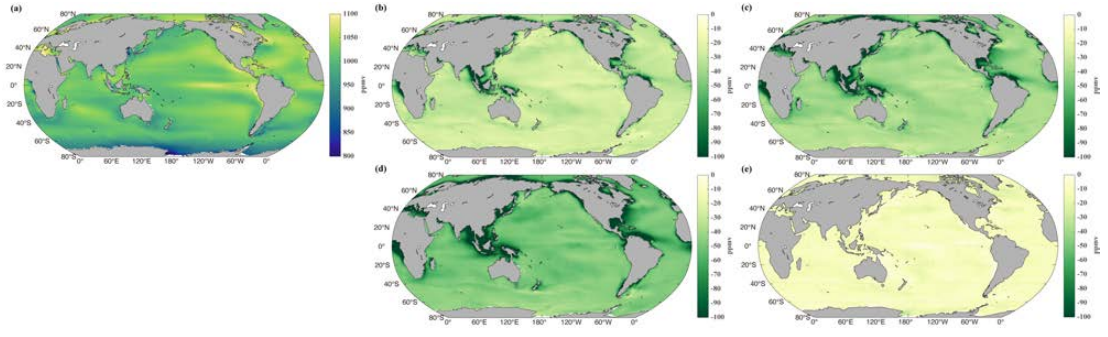

https://doi.org/10.5194/egusphere-2025-2536
Preprint. Discussion started: 23 June 2025

Figure 6: Distribution of surface pCO_2. (a) control simulation, (b) difference between OWE5 and CTL, (c) difference between OWE75 and CTL, (d) difference between OWE10 and CTL, (e) difference between OWE0 and CTL.

3.3 Responses of DIC inventory to alkalinity enhancement

The DIC inventory ($[DIC]_T$) for each column is calculated using the following equation:

$$[DIC]_T = \sum_{i=1}^{n_z} ([DIC]_i \times V_i) ,$$

where $[DIC]_i$ represents DIC concentration with a unit of mmol/m^3, V_i is the volume of the grid box i, n_z is the number of boxes for each column.

OAE-induced CO_2 absorption leads to an increase in the ocean's total DIC inventory, reflecting enhanced carbon storage. In CTL, the global ocean DIC inventory continues to rise throughout the century due to the increasing atmospheric CO_2 partial pressure under the high-emission scenario (Fig. 3d). The OAE treatments (OWE5, OWE75, and OWE10) enable the ocean to sequester significantly more carbon than CTL during the entire OAE phase (Fig. 3d). By 2100, total ocean DIC increases by 5.39, 7.41, and 9.50 Pmol in OWE5, OWE75, and OWE10, respectively, compared to CTL. Even in OWE0, where alkalinity addition is terminated in 2050, the ocean still stores an additional 2.06 Pmol of DIC relative to the control.

Spatially, DIC inventory increases across most of the ocean in the CTL simulation due to elevated atmospheric CO_2 (Fig. 7a). However, the increase is not uniform—subtropical gyres, particularly those outside the North Pacific, exhibit the strongest DIC gains. In the OAE scenarios, DIC inventory increases further across nearly all ocean basins compared to CTL (Fig. 7b–d). The largest DIC increases occur in the North Atlantic, the South Subtropical Atlantic, and the Indian Ocean, where inventories rise by more than 0.1 Tmol by 2100 under all three OAE treatments. In the North Pacific, DIC increases most notably north of the Kuroshio and its extension. As more alkalinity is added in OWE75 and OWE10, the DIC increase spreads more broadly across the oceans compared to OWE5. In contrast, the Southern Pacific exhibits only a modest increase, and the Southern Ocean and Equatorial Pacific show the least change. Despite the early termination of alkalinity addition in OWE0, DIC inventory still rises across the global ocean, with the most pronounced increase occurring in the North Atlantic (Fig. 7e). However, DIC gains in OWE0 are notably smaller in the North Pacific, Indian Ocean, and South Atlantic compared to other OAE treatments.

Vertically, changes in DIC concentration mirror those of alkalinity (Figs. 8 and 5). OAE-induced positive DIC anomalies reach depths of 200–500 m in the Southern Hemisphere and penetrate as deep as 700 m in the Northern Hemisphere, extending to 1500 m in the subpolar North under all three OAE treatments (Fig. 8a–c). This pattern corresponds to strong CO_2 absorption in regions

https://doi.org/10.5194/egusphere-2025-2536
Preprint. Discussion started: 23 June 2025

with elevated alkalinity (Fig. 5). The subpolar and polar North also exhibit the steepest vertical DIC gradients, with concentrations varying by more than 100 mmol/m³ from the surface to 200–300 m depth. Although alkalinity addition ends in 2050 in OWE0, this scenario still supports CO_2 uptake (Fig. 8d), with DIC increases exceeding 10 mmol/m³ in the upper ocean and over 30 mmol/m³ in the northern subpolar and polar regions. However, these increases are substantially smaller than those in the other OAE treatments, primarily because the decline in surface alkalinity following termination reduces CO_2 absorption relative to OWE5 (Fig. 8e).

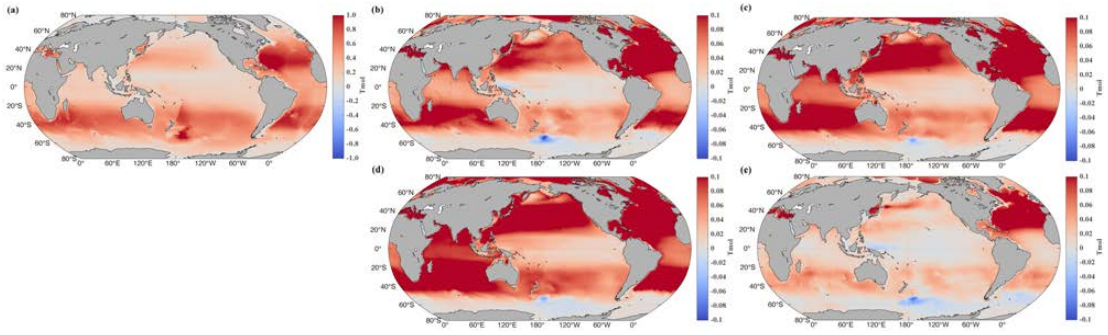

Figure 7: Anomaly of DIC inventory. (a) Change in DIC inventory at the end of the century relative to the initial year, (b) difference between OWE5 and CTL, (c) difference between OWE75 and CTL, (d) difference between OWE10 and CTL, and (e) difference between OWE0 and CTL.

https://doi.org/10.5194/egusphere-2025-2536
Preprint. Discussion started: 23 June 2025

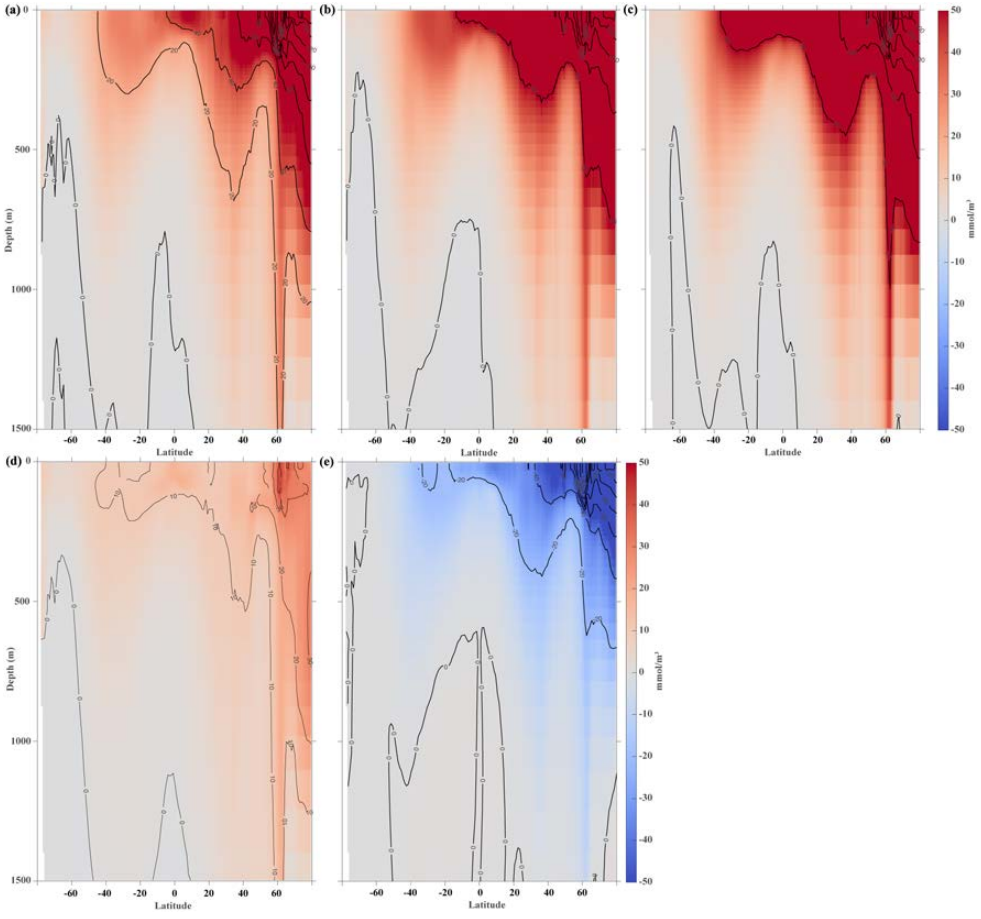

Figure 8. Vertical distribution of DIC inventory anomalies (upper 1500 m). (a) differences between OWE5 and CTL, (b) difference between OWE75 and CTL, (c) difference between OWE10 and CTL, (d) differences between OWE0 and CTL, and (e) differences between OWE0 and OWE5.

3.4 Responses of surface pH to alkalinity enhancement

OAE treatments lead to an increase in surface ocean pH, partially mitigating ocean acidification compared to the control simulation. However, they do not reverse the long-term declining pH trend throughout the 21st century (Fig. 3e). Under the high-emission SSP585 scenario, surface pH declines rapidly from a relatively healthy level (pH = 8.03) to a more acidic state (pH = 7.67) by 2100. The OWE5 treatment consistently alleviates acidification, resulting in a pH increase of 0.02 relative to the control by the end of the century. Stronger alkalinity enhancements in OWE75 and OWE10 yield even greater buffering effects, increasing surface pH by 0.03 and 0.04, respectively. In contrast, OWE0—which terminates alkalinity addition in 2050—results in a much smaller pH increase of only 0.006 by 2100 compared to the control.

https://doi.org/10.5194/egusphere-2025-2536
Preprint. Discussion started: 23 June 2025

Globally, the ocean becomes more acidic by the end of the century under the SSP585 scenario due to continued atmospheric CO_2 uptake (Fig. 9a). The OAE treatments mitigate acidification on a global scale, with the most substantial pH increases observed in coastal regions where riverine alkalinity input is strongest (Fig. 9b–d). In the open ocean, the Atlantic and Indian Oceans show the most notable surface pH increases, while the Southern Ocean and the Pacific exhibit more modest changes. As expected, greater alkalinity additions correspond to stronger pH buffering. Although alkalinity input ceases in OWE0, this scenario still shows a slight increase in surface pH compared to the control, particularly in the Subpolar North Atlantic (SPNA) (Fig. 9e). However, this increase is considerably smaller than those observed in the continuous OAE treatments.

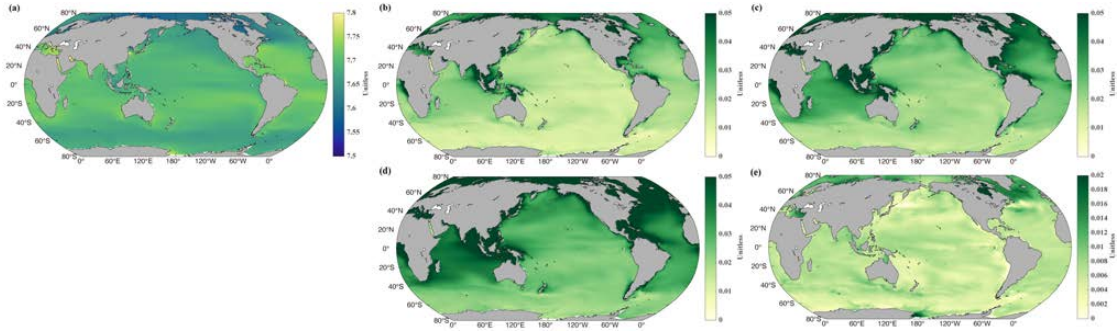

Figure 9: Distribution of surface pH. (a) control simulation at the end of the century, (b) difference between OWE5 and CTL, (c) difference between OWE75 and CTL, (d) difference between OWE10 and CTL, (e) difference between OWE0 and CTL. Note the different colour scale in (e).

3.5 Responses of surface air temperature to alkalinity enhancement

To figure out how OAE can mitigate global warming, we calculate the surface air temperature in all simulations. There is a continuous increase in temperature under CTL, indicating that the temperature keeps rising under the high-emission scenario (Fig. 3f). All the four OAE treatments show a decrease of temperature, with 0.45 °C in OWE5, 0.39 °C in OWE75, 0.34 °C in OWE10, and 0.31 °C in OWE0 compared to CTL by the end of this century (Fig. 3f).

4 Discussion

4.1 The effectiveness of OAE via rivers

The long-standing negative feedback between terrestrial weathering and the oceanic carbon sink—mediated through riverine alkalinity input—makes river-based OAE a practical and feasible carbon removal strategy. In our simulations, we apply 0.088, 0.14, and 0.20 Pmol of excess alkalinity per year at river mouths, representing 5-, 7.5-, and 10-fold increases in alkalinity fluxes due to enhanced weathering. These treatments lead to reductions in atmospheric

https://doi.org/10.5194/egusphere-2025-2536
Preprint. Discussion started: 23 June 2025

CO_2 of 29, 40, and 51 ppm, respectively, which are consistent with the range reported in previous modeling studies. For example, Ilyina et al. (2013) show that doubling the amount of alkalinity relative to CO_2 emissions could lower atmospheric CO_2 by up to 490 ppm. Similarly, González and Ilyina (2016) demonstrate that adding 114 Pmol of alkalinity to the surface ocean under the RCP8.5 scenario could stabilize atmospheric CO_2 at RCP4.5 levels (~520 ppm). While the magnitude of alkalinity addition in these studies is equivalent to 100 times the present-day weathering rate—ten times higher than in our OWE10 scenario—the resulting atmospheric CO_2 reductions are also nearly tenfold greater. In our simulation, a total of 12.64 Pmol of alkalinity added over 80 years yields a 51 ppm CO_2 reduction. Likewise, an alkalinity addition of 0.25 Pmol yr^{-1} lead to an 82-86 ppm decline in atmospheric CO_2 under a high emission scenario, and a 53-58 ppm decline under a low emission scenario (Lenton et al., 2018). Our OWE75 simulation, which adds 0.14 Pmol yr-1 via rivers, achieved a 40 ppm reduction, roughly half the CO_2 drawdown observed in Lenton et al. (2018), in line with the halved addition rate. These comparisons suggest a robust linear relationship between the amount of alkalinity added and the resulting atmospheric CO_2 reduction. However, further research is needed to confirm the consistency and limits of this relationship. Furthermore, Schwinger et al. (2024) suggest that the efficiency of CO_2 drawdown via OAE is influenced by the emission pathway, with greater declines under high-emission scenarios compared to low-emission ones. Therefore, under lower-emission scenarios, the CO_2 reduction achieved through riverine OAE is likely to be less pronounced than what we observe under the SSP585 scenario.

We calculate additional DIC stored per unit of TA added, referred to as absorption efficiency, following the definition by Palmiéri and Yool (2024). By the end of the century, the OAE simulations result in DIC inventory increases of 5.39, 7.41, and 9.50 Pmol in the OWE5, OWE75, and OWE10 simulations, respectively. These correspond to absorption efficiencies of 0.77, 0.77, and 0.75. Our results fall within the range reported in previous studies (0.46 – 0.95). The wide range in previous studies is probably due to spatial and temporal variability, as well as differences in OAE application methods. Our results are consistent with Palmiéri and Yool (2024), who reported a global mean absorption efficiency of 0.78 when OAE is applied in shallow continental shelves. In our simulations, the Southern Ocean exhibits the smallest increase in DIC due to its distance from the riverine alkalinity sources. However, when OAE is applied specifically in the Southern Ocean, higher absorption efficiencies have been reported compared to uniform global deployment (Burt et al., 2021). This suggests that the Southern Ocean may be a particularly effective region for OAE, but further studies are needed to confirm its potential.

Using a simple carbon cycle box-model, Köhler (2020) showed that the absorption efficiency gradually increases to a peak value of 0.81 at the time of maximum atmospheric CO_2 emissions, then declines to half of that peak after a 2000-year simulation, due to carbonate chemistry and sedimentary processes. In a relative short-term simulation, a gradual increase in absorption efficiency is observed when alkalinity is added in coastal regions (He & Tyka, 2023). In our

https://doi.org/10.5194/egusphere-2025-2536
Preprint. Discussion started: 23 June 2025

three OAE simulations (OWE5, OWE75, and OWE10), absorption efficiency increases from 0.2 in the first year to 0.77, 0.77, and 0.75 by the end of the century, respectively, which are consistent with those of He and Tyka (2023). Both our study and that of He and Tyka (2023) likely missed the later decline in absorption efficiency reported by Köhler (2020), due to the shorter simulation times. Additionally, we find that absorption efficiency is slightly lower in simulations where more alkalinity is added. For example, the efficiency in OWE10 is 0.75, compared to 0.77 in both OWE5 and OWE75, indicating a trade-off between the amount of alkalinity added and the resulting efficiency. In practice, it is essential to identify optimal deployment strategies that maximize efficiency while minimizing cost.

4.2 OAE distribution affected by circulations

Although alkalinity is introduced via rivers, its effects extend to the open oceans, with more pronounced impacts observed in the Atlantic and Indian Oceans compared to the Pacific (Fig. 3). This pattern is likely driven by differences in ocean topography and circulation. For instance, in the Atlantic, excess alkalinity from the Caribbean Sea can be transported to the North Atlantic by the Gulf Stream, a strong western boundary current. In contrast, in the Pacific, the Kuroshio Current is obstructed by island chains, limiting the spread of high-alkalinity waters into the wider Pacific. As a result, the North Atlantic receives a greater supply of alkalinity. Moreover, our findings differ from those of Zhou et al. (2024), who simulate higher absorption efficiency in the equatorial Pacific compared to the subtropical regions. In our simulations, the equatorial Pacific shows only minimal increases in DIC inventory. We attribute this to the location of alkalinity addition. In the eastern equatorial Pacific, estuaries that could contribute to OAE are sparce and have low alkalinity fluxes. Consequently, the limited supply of alkalinity to this region leads to a negligible increase in DIC within the equatorial upwelling zones. These results highlight that the location of alkalinity addition plays a critical role in shaping the spatial distribution of OAE effectiveness.

The vertical distribution of excess alkalinity further illustrates the influence of meridional circulation on OAE. The most affected region is the SPNA, where excess alkalinity penetrates to depths greater than 1500 m due to deep-water formation (Fig. 4a). In both the north and south subtropical gyres, the downward sloping of isoclines indicates a convergent effect that facilitates the subduction of alkalinity. In equatorial regions, the positive alkalinity anomaly remains shallower than in the subtropical gyres, suggesting that upwelling in these regions retains excess alkalinity near the surface. This pattern aligns with the findings of Lenton et al. (2018). It is important to note that OAE occurring in deep-water formation or convergence regions does not necessarily imply lower efficiency. Nagwekar et al. (2024) demonstrate through modeling that mCDR in these regions remains effective and holds significant potential.

4.3 Challenges of OAE

One of the most critical challenges in OAE is the removal of alkalinity through precipitation, which can rapidly reduce water column alkalinity and significantly lower the efficiency of OAE

https://doi.org/10.5194/egusphere-2025-2536
Preprint. Discussion started: 23 June 2025

(Moras et al., 2022). Key factors influencing alkalinity loss include the type of mineral used, the form of added alkalinity, the solution state (equilibrated vs. non-equilibrated), and the presence of particles (Hartmann et al., 2023). To mitigate particle-induced precipitation, it is crucial to consider both the type of alkaline material and its surface chemistry. CO_2-equilibrated alkaline solutions, such as $NaHCO_3$ and Na_2CO_3, have been proposed as promising alternatives because they help maintain the carbonate system near saturation threshold while minimizing ecological impacts (González-Santana et al., 2024; Marín-Samper et al., 2024; Xin et al., 2024). These solutions are less likely to trigger precipitation and have been recommended for OAE applications (Hartmann et al., 2023; Suitner et al., 2024). Magnesium (Mg)-based minerals have also been proposed for OAE, as the present of Mg can inhibit $CaCO_3$ precipitation and thus help preserve alkalinity (Jones, 2017; Pan et al., 2021). However, the most widely used Mg-rich mineral, olivine, has been shown to cause significant alkalinity loss through precipitation, making it less efficient for carbon uptake than previous assumed (Fuhr et al., 2022). Köhler et al. (2013) recommended using particles with a grain size of 1 μm to ensure slow sinking and complete dissolution. However, the energy required for grinding particles to this size can reduce overall carbon sequestration efficiency. Furthermore, particles present in river plumes can act as nucleation sites for carbonate precipitation and initiate heterogeneous reactions, leading to substantial losses of DIC and alkalinity (Wurgaft et al., 2021). Thus, when implementing OAE through river systems, the amount of added alkalinity must be carefully regulated to avoid significant loss in estuarine regions due to $CaCO_3$ precipitation.

Meeting the substantial material requirements for OAE materials presents another major challenge. To achieve annual OAE rate of 0.088, 0.14 and 0.20 Pmol, and assuming that each mole of olivine releases 4 moles of alkalinity with a mole mass of 140 g mol^{-1} (Feng et al., 2017), approximately 3.08, 4.9, and 7 billion tons of olivine would be required per year, respectively. The current global production of olivine at only 8.4 million tons annually - far below the required amount (Caserini et al., 2022). Industrial by-products such as slag, cement, and lime could partially offset this shortfall. These materials collectively represent around 7 billion tons of alkaline output annually and have a CO_2 storage potential of 2.9-8.5 billion tons per year (Renforth, 2019). Thus, they offer a promising supplemental source of alkalinity for OAE. Restoration of blue carbon ecosystems may also contribute additional alkalinity. For instance, mangrove restoration can enhance respiration and sediment dissolution, increasing local alkalinity levels (Fakhraee et al., 2023). However, the overall magnitude and long-term effectiveness of this approach remain uncertain and warrant further investigation.

Several additional concerns deserve attention. Bach (2024) raised the issue of “additionality”, where anthropogenic alkalinity inputs may reduce the dissolution of natural alkalinity sources. This highlights the need for further study of interactions between natural and artificial alkalinity sources under OAE scenarios. Furthermore, González et al. (2018) found that warming and acidification rates can accelerate following the cessation of alkalinity enhancement, suggesting that long-term deployment strategies are necessary to avoid abrupt climate rebound effects. Our

https://doi.org/10.5194/egusphere-2025-2536
Preprint. Discussion started: 23 June 2025

own simulations also show a rapid decline in pH and CO_2 uptake after alkalinity addition ceases, underscoring the importance of sustained application.

Importantly, OAE at the levels of alkalinity addition used in our study is insufficient to reverse the trajectory of climate change. Under the SSP585 scenario, global temperature keeps increasing even with OAE interventions. While OAE treatments slightly reduce surface temperature, they fail to halt the overall warming trend. These results are consistent with Lenton et al. (2018), who found that uniform global alkalinity addition under the RCP8.5 scenario produced only modest climate effects. Therefore, in high-emission scenarios, increasing ocean alkalinity may help mitigate ocean acidification but is unlikely to substantially reduce global temperatures. Additional carbon dioxide removal (CDR) strategies, such as solar radiation management (SRM), may be required to avoid dangerous temperature overshoot.

5 Conclusions and unresolved problems

In this study, we evaluated the efficacy of ocean alkalinity enhancement (OAE) using the CESM-MARBL model under a high-emission scenario, employing an idealized method of alkalinity addition. Although the model's spatial resolution is relatively coarse for capturing the complex physical processes in coastal regions, the riverine source and sink terms have been extensively calibrated against observational data. Furthermore, our simulations do not alter the model's physical dynamics; only the magnitude of alkalinity inputs is modified. Therefore, we believe that the impact of model resolution on our results is minimal. To focus on the theoretical potential of OAE, we simulated the addition of "pure alkalinity." However, real-world applications must contend with challenges such as alkalinity precipitation, particularly runaway precipitation. Future OAE modeling efforts should incorporate additional constraints and empirical formulations to better represent the behavior of actual alkaline particles (Fennel et al., 2023).

Our findings show that even a tenfold increase in alkalinity flux is insufficient to reverse the trends of ocean acidification or rising atmospheric CO_2 levels under a high-emission scenario. This underscores the urgent need for complementary technological innovations and aggressive emission reduction strategies to curb CO_2 emissions. In parallel, other CDR techniques will be necessary to actively draw down atmospheric CO_2. Additionally, in our OWE0 simulation, if alkalinity addition ceases in 2050, the ocean continues to absorb atmospheric CO_2, though at a reduced rate compared to scenarios where alkalinity addition persists through the end of the century.

https://doi.org/10.5194/egusphere-2025-2536
Preprint. Discussion started: 23 June 2025

Author Contributions

W.-L. W. conceived the project. X.-Y. Z carried out the formal analyses with inputs from W.-L. W and S. L. X.-Y. Z., W.-L. W., and S. L. wrote the manuscript. All authors have given approval to the final version of the manuscript.

Code/Data availability

There is no new code created in this study. Data are available at the following repository https://doi.org/10.5281/zenodo.15550663

Competing interests

The authors declare that there is no competing interests.

Acknowledgments

We thank the hundreds of scientists and researchers who built and has been maintaining the Community Earth System Model. W.-L.W and X.-Y.Z. were supported by the National Natural Science Foundation of China (42476031), the National Key Research and Development Program of China (NKPs) 2023YFF0805004 and the Natural Science Foundation of Fujian Province of China 2023J02001.

References

Bach, L. T. (2024). The additionality problem of ocean alkalinity enhancement. *Biogeosciences*, *21*(1), 261-277. https://doi.org/10.5194/bg-21-261-2024

Bach, L. T., Tamsitt, V., Baldry, K., McGee, J., Laurenceau-Cornec, E. C., Strzepek, R. F., Xie, Y., & Boyd, P. W. (2023). Identifying the Most (Cost-)Efficient Regions for CO2 Removal With Iron Fertilization in the Southern Ocean. *Global Biogeochemical Cycles*, *37*(11), e2023GB007754. https://doi.org/https://doi.org/10.1029/2023GB007754

Beaufort, L., Probert, I., de Garidel-Thoron, T., Bendif, E. M., Ruiz-Pino, D., Metzl, N., Goyet, C., Buchet, N., Coupel, P., Grelaud, M., Rost, B., Rickaby, R. E. M., & de Vargas, C. (2011). Sensitivity of coccolithophores to carbonate chemistry and ocean acidification. *Nature*, *476*(7358), 80-83. https://doi.org/10.1038/nature10295

Beusen, A. H. W., Van Beek, L. P. H., Bouwman, A. F., Mogollón, J. M., & Middelburg, J. J. (2015). Coupling global models for hydrology and nutrient loading to simulate nitrogen and phosphorus retention in surface water – description of IMAGE–GNM and analysis of performance. *Geosci. Model Dev.*, *8*(12), 4045-4067. https://doi.org/10.5194/gmd-8-4045-2015

Burt, D. J., Fröb, F., & Ilyina, T. (2021). The Sensitivity of the Marine Carbonate System to Regional Ocean Alkalinity Enhancement [Original Research]. *Frontiers in Climate*, *3*. https://doi.org/10.3389/fclim.2021.624075

Caserini, S., Storni, N., & Grosso, M. (2022). The Availability of Limestone and Other Raw Materials for Ocean Alkalinity Enhancement. *Global Biogeochemical Cycles*, *36*(5), e2021GB007246. https://doi.org/https://doi.org/10.1029/2021GB007246

https://doi.org/10.5194/egusphere-2025-2536
Preprint. Discussion started: 23 June 2025

Chikamoto, M. O., DiNezio, P., & Lovenduski, N. (2023). Long-Term Slowdown of Ocean Carbon Uptake by Alkalinity Dynamics. *Geophysical Research Letters*, *50*(4), e2022GL101954. https://doi.org/https://doi.org/10.1029/2022GL101954

Danabasoglu, G., Lamarque, J.-F., Bacmeister, J., Bailey, D. A., DuVivier, A. K., Edwards, J., Emmons, L. K., Fasullo, J., Garcia, R., Gettelman, A., Hannay, C., Holland, M. M., Large, W. G., Lauritzen, P. H., Lawrence, D. M., Lenaerts, J. T. M., Lindsay, K., Lipscomb, W. H., Mills, M. J., . . . Strand, W. G. (2020). The Community Earth System Model Version 2 (CESM2). *Journal of Advances in Modeling Earth Systems*, *12*(2), e2019MS001916. https://doi.org/https://doi.org/10.1029/2019MS001916

Duarte, C. M., Bruhn, A., & Krause-Jensen, D. (2022). A seaweed aquaculture imperative to meet global sustainability targets. *Nature Sustainability*, *5*(3), 185-193. https://doi.org/10.1038/s41893-021-00773-9

Eisaman, M. D., Geilert, S., Renforth, P., Bastianini, L., Campbell, J., Dale, A. W., Foteinis, S., Grasse, P., Hawrot, O., Löscher, C. R., Rau, G. H., & Rønning, J. (2023). Assessing the technical aspects of ocean-alkalinity-enhancement approaches. *Guide to Best Practices in Ocean Alkalinity Enhancement Research*, *2-oae2023*, 3. https://doi.org/10.5194/sp-2-oae2023-3-2023

Fakhraee, M., Planavsky, N. J., & Reinhard, C. T. (2023). Ocean alkalinity enhancement through restoration of blue carbon ecosystems. *Nature Sustainability*, *6*(9), 1087-1094. https://doi.org/10.1038/s41893-023-01128-2

Feng, E. Y., Koeve, W., Keller, D. P., & Oschlies, A. (2017). Model-Based Assessment of the CO2 Sequestration Potential of Coastal Ocean Alkalinization. *Earth's Future*, *5*(12), 1252-1266. https://doi.org/https://doi.org/10.1002/2017EF000659

Fennel, K., Long, M. C., Algar, C., Carter, B., Keller, D., Laurent, A., Mattern, J. P., Musgrave, R., Oschlies, A., Ostiguy, J., Palter, J. B., & Whitt, D. B. (2023). Modelling considerations for research on ocean alkalinity enhancement (OAE). *Guide to Best Practices in Ocean Alkalinity Enhancement Research*, *2-oae2023*, 9. https://doi.org/10.5194/sp-2-oae2023-9-2023

Friedlingstein, P., O'Sullivan, M., Jones, M. W., Andrew, R. M., Bakker, D. C. E., Hauck, J., Landschützer, P., Le Quéré, C., Luijkx, I. T., Peters, G. P., Peters, W., Pongratz, J., Schwingshackl, C., Sitch, S., Canadell, J. G., Ciais, P., Jackson, R. B., Alin, S. R., Anthoni, P., . . . Zheng, B. (2023). Global Carbon Budget 2023. *Earth Syst. Sci. Data*, *15*(12), 5301-5369. https://doi.org/10.5194/essd-15-5301-2023

Fuhr, M., Geilert, S., Schmidt, M., Liebetrau, V., Vogt, C., Ledwig, B., & Wallmann, K. (2022). Kinetics of Olivine Weathering in Seawater: An Experimental Study [Original Research]. *Frontiers in Climate*, *4*. https://doi.org/10.3389/fclim.2022.831587

Gasser, T., Guivarch, C., Tachiiri, K., Jones, C. D., & Ciais, P. (2015). Negative emissions physically needed to keep global warming below 2 °C. *Nature Communications*, *6*(1), 7958. https://doi.org/10.1038/ncomms8958

González, M. F., & Ilyina, T. (2016). Impacts of artificial ocean alkalinization on the carbon cycle and climate in Earth system simulations. *Geophysical Research Letters*, *43*(12), 6493-6502. https://doi.org/https://doi.org/10.1002/2016GL068576

González, M. F., Ilyina, T., Sonntag, S., & Schmidt, H. (2018). Enhanced Rates of Regional Warming and Ocean Acidification After Termination of Large-Scale Ocean Alkalinization. *Geophysical Research Letters*, *45*(14), 7120-7129. https://doi.org/https://doi.org/10.1029/2018GL077847

González-Santana, D., Segovia, M., González-Dávila, M., Ramírez, L., González, A. G., Pozzo, L. J., Arnone, V., Vázquez, V., Riebesell, U., & Santana-Casiano, J. M. (2023). Ocean alkalinity enhancement using sodium carbonate salts does not impact Fe dynamics in a mesocosm experiment. *EGUsphere*, *2023*, 1-20. https://doi.org/10.5194/egusphere-2023-2868

González-Santana, D., Segovia, M., González-Dávila, M., Ramírez, L., González, A. G., Pozzo-Pirotta, L. J., Arnone, V., Vázquez, V., Riebesell, U., & Santana-Casiano, J. M. (2024). Ocean alkalinity enhancement using sodium carbonate salts does not lead to measurable changes in Fe dynamics in a mesocosm experiment. *Biogeosciences*, *21*(11), 2705-2715. https://doi.org/10.5194/bg-21-2705-2024

Guo, J. A., Strzepek, R. F., Swadling, K. M., Townsend, A. T., & Bach, L. T. (2023). Influence of Ocean Alkalinity Enhancement with Olivine or Steel Slag on a Coastal Plankton Community in Tasmania. *EGUsphere*, *2023*, 1-27. https://doi.org/10.5194/egusphere-2023-2120

Hartmann, J., Suitner, N., Lim, C., Schneider, J., Marín-Samper, L., Arístegui, J., Renforth, P., Taucher, J., & Riebesell, U. (2023). Stability of alkalinity in ocean alkalinity enhancement (OAE) approaches – consequences for durability of CO2 storage. *Biogeosciences*, *20*(4), 781-802. https://doi.org/10.5194/bg-20-781-2023

He, J., & Tyka, M. D. (2023). Limits and CO2 equilibration of near-coast alkalinity enhancement. *Biogeosciences*, *20*(1), 27-43. https://doi.org/10.5194/bg-20-27-2023

https://doi.org/10.5194/egusphere-2025-2536
Preprint. Discussion started: 23 June 2025

Ilyina, T., Wolf-Gladrow, D., Munhoven, G., & Heinze, C. (2013). Assessing the potential of calcium-based artificial ocean alkalinization to mitigate rising atmospheric CO2 and ocean acidification. *Geophysical Research Letters*, *40*(22), 5909-5914. https://doi.org/https://doi.org/10.1002/2013GL057981

IPCC. (2023). Climate Change 2023: Synthesis Report. Contribution of Working Groups I, II and III to the Sixth Assessment Report of the Intergovernmental Panel on Climate Change [Core Writing Team, H. Lee and J. Romero (eds.)]. *Intergovernmental Pannel on Climate Change (IPCC)*. https://doi.org/10.59327/IPCC/AR6-9789291691647.

Jones, B. (2017). Review of calcium carbonate polymorph precipitation in spring systems. *Sedimentary Geology*, *353*, 64-75. https://doi.org/https://doi.org/10.1016/j.sedgeo.2017.03.006

Jones, C. D., Arora, V., Friedlingstein, P., Bopp, L., Brovkin, V., Dunne, J., Graven, H., Hoffman, F., Ilyina, T., John, J. G., Jung, M., Kawamiya, M., Koven, C., Pongratz, J., Raddatz, T., Randerson, J. T., & Zaehle, S. (2016). C4MIP – The Coupled Climate–Carbon Cycle Model Intercomparison Project: experimental protocol for CMIP6. *Geosci. Model Dev.*, *9*(8), 2853-2880. https://doi.org/10.5194/gmd-9-2853-2016

Jürchott, M., Oschlies, A., & Koeve, W. (2023). Artificial Upwelling—A Refined Narrative. *Geophysical Research Letters*, *50*(4), e2022GL101870. https://doi.org/https://doi.org/10.1029/2022GL101870

Keller, D. P., Feng, E. Y., & Oschlies, A. (2014). Potential climate engineering effectiveness and side effects during a high carbon dioxide-emission scenario. *Nature Communications*, *5*(1), 3304. https://doi.org/10.1038/ncomms4304

Kleypas, J. A., Buddemeier, R. W., Archer, D., Gattuso, J.-P., Langdon, C., & Opdyke, B. N. (1999). Geochemical Consequences of Increased Atmospheric Carbon Dioxide on Coral Reefs. *Science*, *284*(5411), 118-120. https://doi.org/doi:10.1126/science.284.5411.118

Köhler, P. (2020). Anthropogenic CO2 of High Emission Scenario Compensated After 3500 Years of Ocean Alkalinization With an Annually Constant Dissolution of 5 Pg of Olivine [Original Research]. *Frontiers in Climate*, *2*. https://www.frontiersin.org/journals/climate/articles/10.3389/fclim.2020.575744

Köhler, P., Abrams, J. F., Völker, C., Hauck, J., & Wolf-Gladrow, D. A. (2013). Geoengineering impact of open ocean dissolution of olivine on atmospheric CO2, surface ocean pH and marine biology. *Environmental Research Letters*, *8*(1), 014009. https://doi.org/10.1088/1748-9326/8/1/014009

Lampitt, R. S., Achterberg, E. P., Anderson, T. R., Hughes, J. A., Iglesias-Rodriguez, M. D., Kelly-Gerreyn, B. A., Lucas, M., Popova, E. E., Sanders, R., Shepherd, J. G., Smythe-Wright, D., & Yool, A. (2008). Ocean fertilization: a potential means of geoengineering? *Philosophical Transactions of the Royal Society A: Mathematical, Physical and Engineering Sciences*, *366*(1882), 3919-3945. https://doi.org/doi:10.1098/rsta.2008.0139

Lenton, A., Matear, R. J., Keller, D. P., Scott, V., & Vaughan, N. E. (2018). Assessing carbon dioxide removal through global and regional ocean alkalinization under high and low emission pathways. *Earth Syst. Dynam.*, *9*(2), 339-357. https://doi.org/10.5194/esd-9-339-2018

Long, M. C., Moore, J. K., Lindsay, K., Levy, M., Doney, S. C., Luo, J. Y., Krumhardt, K. M., Letscher, R. T., Grover, M., & Sylvester, Z. T. (2021). Simulations With the Marine Biogeochemistry Library (MARBL). *Journal of Advances in Modeling Earth Systems*, *13*(12), e2021MS002647. https://doi.org/https://doi.org/10.1029/2021MS002647

Marín-Samper, L., Arístegui, J., Hernández-Hernández, N., Ortiz, J., Archer, S. D., Ludwig, A., & Riebesell, U. (2024). Assessing the impact of CO2-equilibrated ocean alkalinity enhancement on microbial metabolic rates in an oligotrophic system. *Biogeosciences*, *21*(11), 2859-2876. https://doi.org/10.5194/bg-21-2859-2024

Mayorga, E., Seitzinger, S. P., Harrison, J. A., Dumont, E., Beusen, A. H. W., Bouwman, A. F., Fekete, B. M., Kroeze, C., & Van Drecht, G. (2010). Global Nutrient Export from WaterSheds 2 (NEWS 2): Model development and implementation. *Environmental Modelling & Software*, *25*(7), 837-853. https://doi.org/https://doi.org/10.1016/j.envsoft.2010.01.007

Montserrat, F., Renforth, P., Hartmann, J., Leermakers, M., Knops, P., & Meysman, F. J. R. (2017). Olivine Dissolution in Seawater: Implications for CO2 Sequestration through Enhanced Weathering in Coastal Environments. *Environmental Science & Technology*, *51*(7), 3960-3972. https://doi.org/10.1021/acs.est.6b05942

Moras, C. A., Bach, L. T., Cyronak, T., Joannes-Boyau, R., & Schulz, K. G. (2022). Ocean alkalinity enhancement – avoiding runaway CaCO3 precipitation during quick and hydrated lime dissolution. *Biogeosciences*, *19*(15), 3537-3557. https://doi.org/10.5194/bg-19-3537-2022

https://doi.org/10.5194/egusphere-2025-2536
Preprint. Discussion started: 23 June 2025

Nagwekar, T., Nissen, C., & Hauck, J. (2024). Ocean Alkalinity Enhancement in Deep Water Formation Regions Under Low and High Emission Pathways. *Earth's Future*, *12*(10), e2023EF004213. https://doi.org/https://doi.org/10.1029/2023EF004213

Oschlies, A., Bach, L. T., Rickaby, R. E. M., Satterfield, T., Webb, R., & Gattuso, J. P. (2023). Climate targets, carbon dioxide removal, and the potential role of ocean alkalinity enhancement. *Guide to Best Practices in Ocean Alkalinity Enhancement Research*, *2-oae2023*, 1. https://doi.org/10.5194/sp-2-oae2023-1-2023

Palmiéri, J., & Yool, A. (2024). Global-Scale Evaluation of Coastal Ocean Alkalinity Enhancement in a Fully Coupled Earth System Model. *Earth's Future*, *12*(3), e2023EF004018. https://doi.org/https://doi.org/10.1029/2023EF004018

Pan, Y., Li, Y., Ma, Q., He, H., Wang, S., Sun, Z., Cai, W.-J., Dong, B., Di, Y., Fu, W., & Chen, C.-T. A. (2021). The role of Mg2+ in inhibiting CaCO3 precipitation from seawater. *Marine Chemistry*, *237*, 104036. https://doi.org/https://doi.org/10.1016/j.marchem.2021.104036

Renforth, P. (2019). The negative emission potential of alkaline materials. *Nature Communications*, *10*(1), 1401. https://doi.org/10.1038/s41467-019-09475-5

Renforth, P., & Henderson, G. (2017). Assessing ocean alkalinity for carbon sequestration. *Reviews of Geophysics*, *55*(3), 636-674. https://doi.org/https://doi.org/10.1002/2016RG000533

Riebesell, U., Zondervan, I., Rost, B., Tortell, P. D., Zeebe, R. E., & Morel, F. M. M. (2000). Reduced calcification of marine plankton in response to increased atmospheric CO2. *Nature*, *407*(6802), 364-367. https://doi.org/10.1038/35030078

Schwinger, J., Bourgeois, T., & Rickels, W. (2024). On the emission-path dependency of the efficiency of ocean alkalinity enhancement. *Environmental Research Letters*. http://iopscience.iop.org/article/10.1088/1748-9326/ad5a27

Smith, R., Jones, P., Briegleb, B., Bryan, F., Danabasoglu, G., Dennis, J., Dukowicz, J., Eden, C., Fox-Kemper, B., & Gent, P. (2010). The parallel ocean program (POP) reference manual ocean component of the community climate system model (CCSM) and community earth system model (CESM). *LAUR-01853*, *141*, 1-140.

Suitner, N., Faucher, G., Lim, C., Schneider, J., Moras, C. A., Riebesell, U., & Hartmann, J. (2024). Ocean alkalinity enhancement approaches and the predictability of runaway precipitation processes: results of an experimental study to determine critical alkalinity ranges for safe and sustainable application scenarios. *Biogeosciences*, *21*(20), 4587-4604. https://doi.org/10.5194/bg-21-4587-2024

Tyka, M. D. (2025). Efficiency metrics for ocean alkalinity enhancements under responsive and prescribed atmospheric pCO2 conditions. *Biogeosciences*, *22*(1), 341-353. https://doi.org/10.5194/bg-22-341-2025

UNFCCC. (2015). Paris Agreement. *United Nations Framework Convention on Climate Change (UNFCCC)*.

Wang, W.-L., Fernández-Méndez, M., Elmer, F., Gao, G., Zhao, Y., Han, Y., Li, J., Chai, F., & Dai, M. (2023). Ocean afforestation is a potentially effective way to remove carbon dioxide. *Nature Communications*, *14*(1), 4339. https://doi.org/10.1038/s41467-023-39926-z

Wurgaft, E., Wang, Z. A., Churchill, J. H., Dellapenna, T., Song, S., Du, J., Ringham, M. C., Rivlin, T., & Lazar, B. (2021). Particle Triggered Reactions as an Important Mechanism of Alkalinity and Inorganic Carbon Removal in River Plumes. *Geophysical Research Letters*, *48*(11), e2021GL093178. https://doi.org/https://doi.org/10.1029/2021GL093178

Xin, X., Goldenberg, S. U., Taucher, J., Stuhr, A., Arístegui, J., & Riebesell, U. (2024). Resilience of Phytoplankton and Microzooplankton Communities under Ocean Alkalinity Enhancement in the Oligotrophic Ocean. *Environmental Science & Technology*, *58*(47), 20918-20930. https://doi.org/10.1021/acs.est.4c09838

Zeebe, R. E., Zachos, J. C., Caldeira, K., & Tyrrell, T. (2008). Carbon Emissions and Acidification. *Science*, *321*(5885), 51-52. https://doi.org/doi:10.1126/science.1159124

Zhou, M., Tyka, M. D., Ho, D. T., Yankovsky, E., Bachman, S., Nicholas, T., Karspeck, A. R., & Long, M. C. (2024). Mapping the global variation in the efficiency of ocean alkalinity enhancement for carbon dioxide removal. *Nature Climate Change*. https://doi.org/10.1038/s41558-024-02179-9